Universal Quantum Computation Using Discrete Holonomies

by

Cornelis Johannes Gerardus Mommers

Supervised by Erik Sjöqvist

Uppsala Universitet

Abstract

Holonomic quantum computation exploits a quantum state's non-trivial, matrix-valued geometric phase to perform fault-tolerant computations. Holonomies arising from systems where the Hamiltonian traces a continuous path through state space have been the subject of a significant amount of research. Discrete holonomies, on the other hand, where the state jumps from point to point, have had little prior investigation. In the context of an interferometry experiment, we build an explicit model for universal quantum computation using a sequence of incomplete projective measurements of the angular momentum operator. We show that quantum gates constructed with discrete holonomies are resilient to errors. In the limit of dense measurements we recover known results from the continuous-path holonomy. Our work sets the stage for verification in the laboratory.

Table of contents

Chapter 1
Introduction

The road to efficient quantum computation is paved with instability and error. This report explores a fault-tolerant scheme of quantum computation based on the geometric phase of a quantum state.

Since the advent of quantum mechanics, quantum states are known to have a (non-measurable) global phase. Later, it was realized that states also have a (measurable) geometric phase [1]. Soon after, this phase was generalized to a non-Abelian – meaning matrix-valued – geometric phase [2].

In the circuit model of quantum computation every calculation is realized using a series of transformations, called gates, on a register of qubits. For the entire computation to happen correctly each gate needs to be resilient to errors. A way of ensuring this is by exploiting these non-Abelian geometric phases (holonomies) to execute the action of a gate [3].

Holonomic quantum computation is most often studied in systems where the Hamiltonian traces a continuous path through state space. There are many ways to achieve this experimentally, from using microwaves on spin qubits [4] to solid-state spins in a nitrogen-vacancy center of a diamond [5]. There has not been as much research in the discrete case, whereby the state jumps from point to point in state space.

We map a part of this unexplored territory by modeling discrete holonomies that arise in an interferometry experiment. It is worthwhile to build up a theoretical framework of the experiment as interferometry is such a ubiquitous technique in quantum physics. Since the discrete holonomy is driven by a sequence of projective measurements, our scheme takes inspiration from one-way, or measurement-based quantum computation, but remains within the realm of holonomic quantum computation.

We will show that gates constructed using the interferometry of angular momentum coherent states can achieve universality – that is, they can approximate any unitary transformation. Both the relevant single- and two-qubit gates will be explicitly constructed. Finally, we show that the limiting case of our experiment reduces to the well-known continuous case.

Compared to scant existing literature, [6] we do not require any auxiliary qubits. Our work was written with experiment in mind, meaning it is easier to directly verify our result in the laboratory.

Chapter 2
Theory

2.1. Projective measurements

We will start by reviewing how a quantum state changes after a projective measurement. Suppose we start with a state $|\psi\rangle$ in a finite, N-dimensional Hilbert space $\mathcal{H}$. A projection into a K-dimensional subspace, p_a, (which is also known as an incomplete measurement if $K \geq 2$) can be realized with a projector P_a. After the projective measurement our state transforms as

$$|\psi\rangle \to \frac{P_a |\psi\rangle}{\sqrt{\langle\psi|P_a|\psi\rangle}}, \tag{2.1}$$

with probability $\langle\psi|P_a|\psi\rangle$ [7].

Each subspace p_a represents a point inside the Grassmann manifold $\mathrm{Gr}_{\mathcal{H}}(K, N)$ and can be spanned by a frame $\mathcal{F}_a = \{|a_k\rangle\}_{k=1}^{K}$. Note that there are infinitely many ways (different frames) to span a subspace. The collection of frames form a Stiefel manifold, so each subspace is a fiber and the Stiefel manifold is a fiber bundle with the Grassmann manifold as its base [8]. The overlap matrix, defined component-wise as

$$(\mathcal{F}_a|\mathcal{F}_b)_{kl} := \langle a_k|b_l\rangle\,,$$

quantifies how different subspaces are connected [9]. A series of points inside the Grassmann manifold, $\mathcal{C}$, can be identified with a series of rank-K projections. As these points are also a collection of fibers, $\mathcal{C}$ is a manifestly geometric quantity, and given by

$$\Gamma_{\mathcal{C}} := P_m \dots P_1.$$

We can generalize (2.1) to see how a state changes under the action of $\Gamma_{\mathcal{C}}$. We have that

$$|\psi\rangle \to \frac{\Gamma_{\mathcal{C}} |\psi\rangle}{\sqrt{\langle\psi|P_1 \dots P_{m-1} P_m P_{m-1} \dots P_1|\psi\rangle}}$$

with a probability of $\langle\psi|P_1 \dots P_{m-1} P_m P_{m-1} \dots P_1|\psi\rangle$.

2.2. Experimental setup

We are now at a point where we can build the framework needed to describe a non-Abelian holonomy acquired by a state in a two-path interferometer. Our exposition is based on [10]. The setup is pictured in figure 2.1. A beam of particles with the internal state $|1_k\rangle \in \mathcal{F}_1$ (normalized to unity) is sent through a 50-50 beamsplitter giving the state

$$|\Psi_k\rangle = |1_k\rangle \otimes \frac{1}{\sqrt{2}}(|0\rangle + |1\rangle),$$

where $|0\rangle$ and $|1\rangle$ denote the interferometer arms. In the 1 arm a unitary V, restricted to act unitarily on p_1, is applied. In the 0 arm $|1_k\rangle$ is exposed to a sequence of m projective filtering measurements, $\Gamma_{\mathcal{C}}$. The sequence corresponds to the operators $\Pi_a = P_a \otimes |0\rangle\langle 0| + I \otimes |1\rangle\langle 1|$ for $a = 1, \ldots, m$. The two arms meet at another 50-50 beamsplitter, and the state after the beamsplitter is given by

$$\begin{aligned} |\Psi_k\rangle &= \frac{1}{2}\Gamma_{\mathcal{C}} |1_k\rangle \otimes (|0\rangle + |1\rangle) + \frac{1}{2} V |1_k\rangle \otimes (|0\rangle - |1\rangle) \\ &= \frac{1}{2}(\Gamma_{\mathcal{C}} + V) |1_k\rangle \otimes |0\rangle + \frac{1}{2}(\Gamma_{\mathcal{C}} - V) |1_k\rangle \otimes |1\rangle . \end{aligned}$$

The output intensity in the 0 arm is given by

$$\begin{aligned} \mathcal{I}_k &= \frac{1}{4} \langle 1_k | \Big(\Gamma_{\mathcal{C}}^\dagger + V^\dagger \Big) (\Gamma_{\mathcal{C}} + V) | 1_k \rangle \\ &= \frac{1}{4} \Big(\langle 1_k | V^\dagger V | 1_k \rangle + \langle 1_k | V^\dagger \Gamma_{\mathcal{C}} | 1_k \rangle + \langle 1_k | \Gamma_{\mathcal{C}}^\dagger V | 1_k \rangle + \langle 1_k | \Gamma_{\mathcal{C}}^\dagger \Gamma_{\mathcal{C}} | 1_k \rangle \Big) \\ &= \frac{1}{4} \Big(1 + \langle 1_k | \Gamma_{\mathcal{C}}^\dagger \Gamma_{\mathcal{C}} | 1_k \rangle + 2 \operatorname{Re} \langle 1_k | V^\dagger \Gamma_{\mathcal{C}} | 1_k \rangle \Big). \end{aligned}$$

Let us rewrite $\langle 1_k | V^\dagger \Gamma_{\mathcal{C}} | 1_k \rangle$ in a more convenient form. The first subspace is spanned by $|1_k\rangle$ and $K-1$ other vectors $|1_l\rangle$. Therefore (all sums go from 1 to K),

$$\begin{aligned} \langle 1_k | V^\dagger \Gamma_{\mathcal{C}} | 1_k \rangle &= \sum_l \langle 1_k | V^\dagger | 1_l \rangle \, \langle 1_l | \Gamma_{\mathcal{C}} | 1_k \rangle \\ &= \sum_{l,i,\ldots,j} \langle 1_k | V^\dagger | 1_l \rangle \, \langle 1_l | m_i \rangle \ldots \langle 2_j | 1_k \rangle \\ &= \sum_l \langle 1_k | V^\dagger | 1_l \rangle \, [(\mathcal{F}_1 | \mathcal{F}_m)(\mathcal{F}_m | \mathcal{F}_{m-1}) \ldots (\mathcal{F}_2 | \mathcal{F}_1)]_{lk} \\ &= \big(V^\dagger D \big)_{kk}, \end{aligned}$$

where we have defined $\big(V^\dagger\big)_{kl} := \langle 1_k | V^\dagger | 1_l \rangle$ and $D := (\mathcal{F}_1 | \mathcal{F}_m)(\mathcal{F}_m | \mathcal{F}_{m-1}) \ldots (\mathcal{F}_2 | \mathcal{F}_1)$. Hence,

$$\mathcal{I}_k = \frac{1}{4} \Big(1 + \langle 1_k | \Gamma_{\mathcal{C}}^\dagger \Gamma_{\mathcal{C}} | 1_k \rangle \Big) + \frac{1}{2} \operatorname{Re} \big(V^\dagger D \big)_{kk}.$$

The total intensity is

$$\mathcal{I}_{tot} = \sum_{k=1}^{K} \mathcal{I}_k = \frac{1}{4} \Big(K + \operatorname{Tr} \Big(\Gamma_{\mathcal{C}}^\dagger \Gamma_{\mathcal{C}} \Big) \Big) + \frac{1}{2} \operatorname{Re} \big(\operatorname{Tr} \big[V^\dagger D \big] \big).$$

The final step is to find the unitary V that maximizes the intensity, specifically $\operatorname{Re}\big(\operatorname{Tr}\big[V^\dagger D\big]\big)$. It can be shown that this happens when $V = U_D := |D|^{-1} D$, where $|D| = \sqrt{D D^\dagger}$. U_D is the direct holonomy associated with the sequence $\mathcal{C}$ [10].

So, when we send our beam of particles through the interferometer the output state corresponding to the maximum intensity will have been transformed by the holonomy U_D.

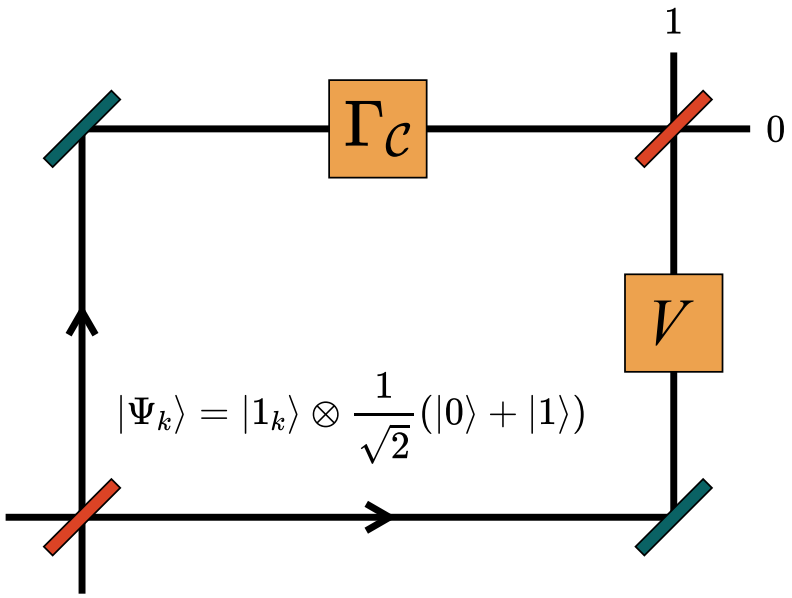

Figure 2.1: The two-path interferometer. The input state gets split by a 50-50 beamsplitter. In one arm the state gets exposed to a series of projections. In the other arm the state undergoes a unitary evolution V. The state in each of the arms meet again at another 50-50 beamsplitter. Adapted from [10].

2.3. Angular momentum coherent states

A particularly interesting class of internal states are the angular momentum coherent states. Let $\{|j,m\rangle\}_{m=-j}^{j}$ be the eigenkets of the J_z operator. The angular momentum coherent states are eigenstates of $J_{\vec{n}}$, the angular momentum operator in the $\vec{n}$ direction, with $m = \pm j$ [11]. Characterizing $\vec{n}$ with spherical coordinates as $(\sin\theta\cos\phi, \sin\theta\sin\phi, \cos\theta)$ the coherent states are $e^{-i\phi J_z}e^{-i\theta J_y}|j,\pm j\rangle$. We always set $\hbar = 1$. Note that $e^{-i\phi\vec{J}\cdot\hat{n}} =: \mathcal{D}_{\vec{n}}(\phi)$ is the rotation operator in the $\vec{n}$ direction. So, the angular momentum coherent states are rotated angular momentum states, where the total rotation has been decomposed into a rotation along the y-axis and then the z-axis.

If $j \geq 1$ we can have our sequence of frames be projections into subspaces spanned by different coherent states, viz.

$$\mathcal{F}(\theta_a, \phi_a) = \left\{e^{-i\phi_a J_z}e^{-i\theta_a J_y}|j,\pm j\rangle\right\} =: \{|\pm j_a\rangle\}.$$

Each projective filtering measurement corresponds to the operator $P_a = |j_a\rangle\langle j_a| + |-j_a\rangle\langle -j_a|$ and represents a measurement of the observable $\left(\vec{n}\cdot\vec{J}\right)^2$ [10].

We can calculate the overlap matrix for the coherent states by decomposing each state into a tensor product of spin-1/2 states, $|\pm j\rangle = \left|\pm\frac{1}{2}\right\rangle^{\otimes 2j}$. The spin-1/2 states must all be $1/2$ or $-1/2$ because we are only looking at states of maximal angular momentum. Hence (where k and l equal $+$ or -, which correspond to the 0 index and to the 1 index of the matrix, respectively),

$$\begin{aligned}
(\mathcal{F}_a|\mathcal{F}_b)_{kl} &= \langle kj|e^{i\theta_a J_y}e^{i\phi_a J_z}e^{-i\phi_b J_z}e^{-i\theta_b J_y}|lj\rangle \\
&= \langle kj|e^{i\theta_a J_y}e^{-i(\phi_b-\phi_a)J_z}e^{-i\theta_b J_y}|lj\rangle \\
&= \langle kj|\mathcal{D}_y(-\theta_a)\mathcal{D}_z(\phi_b-\phi_a)\mathcal{D}_y(\theta_b)|lj\rangle \\
&= \left\langle k\frac{1}{2}\right|^{\otimes 2j}\left(\mathcal{D}_y(-\theta_a)\mathcal{D}_z(\phi_b-\phi_a)\mathcal{D}_y(\theta_b)\left|l\frac{1}{2}\right\rangle\right)^{\otimes 2j}.
\end{aligned}$$

For spin-1/2 particles the rotation operator has the following representation [12]

$$\mathcal{D}_n(\phi) = e^{-i\phi\vec{J}\cdot\hat{n}} = e^{\frac{-i\vec{\sigma}\cdot\hat{n}\phi}{2}} = \cos\left(\frac{\phi}{2}\right)I - i\sin\left(\frac{\phi}{2}\right)\vec{\sigma}\cdot\hat{n}$$
$$= \begin{pmatrix} \cos\left(\frac{\phi}{2}\right) - in_z\sin\left(\frac{\phi}{2}\right) & (-in_x - n_y)\sin\left(\frac{\phi}{2}\right) \\ (-in_x + n_y)\sin\left(\frac{\phi}{2}\right) & \cos\left(\frac{\phi}{2}\right) + in_z\sin\left(\frac{\phi}{2}\right) \end{pmatrix}.$$

Therefore,

$$\mathcal{D}_y(-\theta_a)\mathcal{D}_z(\phi_b-\phi_a)\mathcal{D}_y(\theta_b) = \begin{pmatrix} \cos\left(\frac{-\theta_a}{2}\right) & -\sin\left(\frac{-\theta_a}{2}\right) \\ \sin\left(\frac{-\theta_a}{2}\right) & \cos\left(\frac{-\theta_a}{2}\right) \end{pmatrix}\begin{pmatrix} e^{-i\left(\frac{\phi_b-\phi_a}{2}\right)} & 0 \\ 0 & e^{i\left(\frac{\phi_b-\phi_a}{2}\right)} \end{pmatrix}\begin{pmatrix} \cos\left(\frac{\theta_b}{2}\right) & -\sin\left(\frac{\theta_b}{2}\right) \\ \sin\left(\frac{\theta_b}{2}\right) & \cos\left(\frac{\theta_b}{2}\right) \end{pmatrix}$$
$$= \begin{pmatrix} \cos\left(\frac{\theta_a-\theta_b}{2}\right)\cos\left(\frac{\phi_a-\phi_b}{2}\right) + i\cos\left(\frac{\theta_a+\theta_b}{2}\right)\sin\left(\frac{\phi_a-\phi_b}{2}\right) & \sin\left(\frac{\theta_a-\theta_b}{2}\right)\cos\left(\frac{\phi_a-\phi_b}{2}\right) - i\sin\left(\frac{\theta_a+\theta_b}{2}\right)\sin\left(\frac{\phi_a-\phi_b}{2}\right) \\ -\sin\left(\frac{\theta_a-\theta_b}{2}\right)\cos\left(\frac{\phi_a-\phi_b}{2}\right) - i\sin\left(\frac{\theta_a+\theta_b}{2}\right)\sin\left(\frac{\phi_a-\phi_b}{2}\right) & \cos\left(\frac{\theta_a-\theta_b}{2}\right)\cos\left(\frac{\phi_a-\phi_b}{2}\right) - i\cos\left(\frac{\theta_a+\theta_b}{2}\right)\sin\left(\frac{\phi_a-\phi_b}{2}\right) \end{pmatrix}$$
$$= \begin{pmatrix} A & B \\ -B^* & A^* \end{pmatrix} \in SU(2).$$

So, we find that the overlap matrix is

$$(\mathcal{F}_a|\mathcal{F}_b) = \begin{pmatrix} R_{a,b} & S_{a,b} \\ (-1)^{2j}S^*_{a,b} & R^*_{a,b} \end{pmatrix}$$

with

$$R_{a,b} = \left[\cos\left(\frac{\theta_a-\theta_b}{2}\right)\cos\left(\frac{\phi_a-\phi_b}{2}\right) + i\cos\left(\frac{\theta_a+\theta_b}{2}\right)\sin\left(\frac{\phi_a-\phi_b}{2}\right)\right]^{2j},$$
$$S_{a,b} = \left[\sin\left(\frac{\theta_a-\theta_b}{2}\right)\cos\left(\frac{\phi_a-\phi_b}{2}\right) - i\sin\left(\frac{\theta_a+\theta_b}{2}\right)\sin\left(\frac{\phi_a-\phi_b}{2}\right)\right]^{2j}.$$

Note that $|R(a,b)|^{1/j} + |S(a,b)|^{1/j} = 1$ [10]. Therefore the determinant of the overlap matrix is never zero, meaning the matrix is invertible and hence full rank. So, none of the coherent-state subspaces are orthogonal; assuming j is a half-odd integer we can make a left-polar decomposition of the overlap matrix into

$$(\mathcal{F}_a|\mathcal{F}_b) = |(\mathcal{F}_a|\mathcal{F}_b)|U_{a,b} = \sqrt{|R_{a,b}|^2 + |S_{a,b}|^2}U_{a,b},$$

where $U_{a,b}$ is a unique unitary matrix [10]. We stress that this requires j to be a half-odd integer. If j is an integer then the prefactor ceases to be a number and becomes a positive-semidefinite matrix instead, which is considerably more complicated.

If we perform a sequence of m measurements into the coherent-state subspaces (j is assumed to be a half-odd integer greater than one from now on) then the final holonomy will be

$$U_D = \frac{(\mathcal{F}_1|\mathcal{F}_m)(\mathcal{F}_m|\mathcal{F}_{m-1})\dots(\mathcal{F}_2|\mathcal{F}_1)}{\sqrt{\left(|R_{1,m}|^2 + |S_{1,m}|^2\right)\left(|R_{m,m-1}|^2 + |S_{m,m-1}|^2\right)\dots\left(|R_{2,1}|^2 + |S_{2,1}|^2\right)}}. \tag{2.2}$$

2.4. Quantum gates

Our goal is to manipulate the holonomy to do quantum computations – to find holonomies that correspond to the action of different (unitary) quantum gates. Important single-qubit gates are the Pauli gates (also named σ_x, σ_y and σ_z.):

$$X = \begin{pmatrix} 0 & 1 \\ 1 & 0 \end{pmatrix}, \quad Y = \begin{pmatrix} 0 & -i \\ i & 0 \end{pmatrix}, \quad Z = \begin{pmatrix} 1 & 0 \\ 0 & -1 \end{pmatrix},$$

as well as the Hadamard gate (H), the phase gate (S) and the $\pi/8$ gate (T)

$$H = \frac{1}{\sqrt{2}}\begin{pmatrix}1 & 1\\ 1 & -1\end{pmatrix}, \quad S = \begin{pmatrix}1 & 0\\ 0 & i\end{pmatrix}, \quad T = \begin{pmatrix}1 & 0\\ 0 & e^{i\pi/4}\end{pmatrix}.$$

The CNOT gate acts on two qubits and is represented by

$$\text{CNOT} = \begin{pmatrix}1 & 0 & 0 & 0\\ 0 & 1 & 0 & 0\\ 0 & 0 & 0 & 1\\ 0 & 0 & 1 & 0\end{pmatrix}.$$

It can be shown that the set H, S, T and CNOT can approximate any unitary operation. That is, the set is universal [7].

We can also decompose any single-qubit unitary operation exactly into $\mathcal{D}_z(\alpha)\mathcal{D}_y(\beta)\mathcal{D}_z(\gamma)$ [12]. Here we ignore any additional global phase factors.

2.5. The quantum Zeno effect

By now our strategy should be clear. We want to find those sequences of projections into subspaces of coherent states with $j = (2m+1)/2$, $m \in \mathbb{N}$, that correspond to the action of quantum gates. Our qubit is defined with $|0\rangle = |j\rangle$ and $|1\rangle = |-j\rangle$. This way, we can use the interferometry setup to do quantum computations. However, with each projection into a subspace, there is also a non-zero probability the state collapses into the orthogonal subspace. It is a well-known result that taking the limit of infinitely many projective measurements 'freezes' the system. The quantum Zeno effect can even drive the system through different subspaces with effective certainty [13]. Why, then, do we consider sequences of discrete measurements?

The pragmatic answer is that fewer measurements are experimentally more feasible. There is also a more fundamental reason, though. For our choice of angular momentum coherent states when we take the limit to dense measurements we find that we can only implement a phase gate. To see why, let us divide the total angles into into N steps, $\delta\theta = \theta/N$ and $\delta\phi = \phi/N$, and then take the limit $N \to \infty$. Then, one of the overlap matrices $(\mathcal{F}(\theta_a + \delta\theta, \phi_a + \delta\phi)|\mathcal{F}(\theta_a, \phi_a))$ will contain (up to and including first order)

$$\begin{aligned}
e^{i(\theta_a+\delta\theta)J_y}e^{i(\phi_a+\delta\phi)J_z}e^{-i\phi_a J_z}e^{-i\theta_a J_y} &= e^{i\delta\theta J_y}e^{i\theta_a J_y}e^{i\delta\phi J_z}e^{-i\theta_a J_y}\\
&= (1+i\delta\theta J_y)e^{i\theta_a J_y}(1+i\delta\phi J_z)e^{-i\theta_a J_y}\\
&= (1+i\delta\theta J_y)\big(1+i\delta\phi e^{i\theta_a J_y}J_y e^{-i\theta_a J_y}\big)\\
&= (1+i\delta\theta J_y)(1+i\delta\phi[-\sin(\theta_a)J_x+\cos(\theta_a)J_z])\\
&= 1+i\delta\theta J_y + i\delta\phi(-\sin(\theta_a)J_x+\cos(\theta_a)J_z),
\end{aligned}$$

where when going from the third line to the fourth line we expanded the exponentials and used the commutation relationships for J_i. Using ladder operators we rewrite the above to

$$1+i\delta\theta J_y + i\delta\phi(-\sin(\theta_a)J_x+\cos(\theta_a)J_z) = 1+i\delta\theta\frac{1}{2i}(J_+ - J_-) + i\delta\phi\bigg(-\sin(\theta_a)\frac{1}{2}(J_+ + J_-) + \cos(\theta_a)J_z\bigg).$$

Since $j > 1/2$ the matrix elements with ladder operators will always vanish. The off-diagonal elements will be zero and the diagonal elements will be $1 \pm ij\cos(\theta_a)\delta\phi$. Therefore, in the limit $N \to \infty$ the total holonomy can only be a phase. We have shown that in order to get a non-commuting holonomy with the coherent states, necessary for universality, we require a finite number of projections.

Chapter 3
Results

3.1. Subtleties and starting assumptions

A cursory glance at (2.2) reveals that the relationship between the input angles (the different coherent states) and the final holonomy is complex. Furthermore, different paths through our space can yield the same results. Hence, our first step is to reduce the problem to something more manageable.

To make the holonomy unambiguous we require that the overlap matrix is unitary [10]. So, we restrict j to $j = (2m+1)/2,\ m \in \mathbb{N}$. Our input state will be $|\psi\rangle = a\,|j\rangle + b\,|-j\rangle$ with $|a|^2 + |b|^2 = 1$ and $|\pm j\rangle \in \mathcal{F}_1$, where $\mathcal{F}_1$ spans the first subspace.

To simplify the problem even more we will only consider sequences of four measurements, which is the minimum number of measurements that can yield a non-trivial holonomy. The first measurement is a projection into the same subspace and frame as $|\psi\rangle$. In an experimental setting we can interpret this projection as the preparation of our state into the correct subspace. We then carry out two more projections into subspaces that are different from the first subspace. Finally, we project back into the same subspace and frame as the starting measurement. Without loss of generality we define $(\theta_1, \phi_1) = (\theta_4, \phi_4) =: (0, 0)$. Our sequence of measurements becomes

$$(0,0) \to (\theta_2, \phi_2) \to (\theta_3, \phi_3) \to (0,0).$$

The holonomy, given by (2.2), reduces to

$$\begin{aligned} U_D &= \frac{(\mathcal{F}_1|\mathcal{F}_4)(\mathcal{F}_4|\mathcal{F}_3)(\mathcal{F}_3|\mathcal{F}_2)(\mathcal{F}_2|\mathcal{F}_1)}{\sqrt{\left(|R_{1,4}|^2 + |S_{1,4}|^2\right)\left(|R_{4,3}|^2 + |S_{4,3}|^2\right)\left(|R_{3,2}|^2 + |S_{3,2}|^2\right)\left(|R_{2,1}|^2 + |S_{2,1}|^2\right)}} \\ &= \frac{(\mathcal{F}_4|\mathcal{F}_3)(\mathcal{F}_3|\mathcal{F}_2)(\mathcal{F}_2|\mathcal{F}_1)}{\sqrt{\left(|R_{4,3}|^2 + |S_{4,3}|^2\right)\left(|R_{3,2}|^2 + |S_{3,2}|^2\right)\left(|R_{2,1}|^2 + |S_{2,1}|^2\right)}}, \end{aligned}$$

and the maximum-intensity output state will be $U_D\,|\psi\rangle$.

An astute reader might raise objections to our use of $(0,0)$ as our starting state. Because we have parametrized the direction of the angular momentum with spherical coordinates (and, in extension, our eigenstates), the coordinate ϕ is undefined at the poles, meaning our coherent states are ill-defined as well; at the poles we have $e^{-i\phi J_z}\,|\pm j\rangle$ and $e^{-i\phi J_z} e^{-i\pi J_y}\,|\pm j\rangle$, respectively, so there is no unique eigenstate. In the continuous-path case one can pick coordinates that remove one (but not both) of the singularities [14]. The two patches that cover the system are related by a gauge transformation, and the analysis is strikingly similar to how one would approach a Dirac monopole [15]. In the discrete case we can afford to be slightly more blasé about the singularity. We were careful to define the $(0,0)$ label to correspond to our starting and ending subspace and frame, which is unambiguous. Subsequent measurements are projections into rotated versions of the original subspace. Having discussed the more subtle points of setup, we can move on to constructing the gates.

3.2. Phase gates

We first want to implement a phase gate. We can do so as follows: we expand j as $(2m+1)/2$ with $m \geq 1$ and pick $(\theta_2, \phi_2, \theta_3, \phi_3) = (\pi/2, \pi, \pi/2, \varphi)$, where $\varphi \in [0, 2\pi)$. We find

$$U_{D,z} = \frac{1}{\sqrt{\cos^{2+4m}\left(\frac{\varphi}{2}\right) + \sin^{2+4m}\left(\frac{\varphi}{2}\right)}} \begin{pmatrix} z^* & 0 \\ 0 & z \end{pmatrix} =: \begin{pmatrix} e^{-i\phi/2} & 0 \\ 0 & e^{i\phi/2} \end{pmatrix}, \tag{3.1}$$

with

$$z = (-1)^m e^{i(2m+1)\frac{\varphi}{2}} \left((-1)^m \cos^{2m+1}\left(\frac{\varphi}{2}\right) - i \sin^{2m+1}\left(\frac{\varphi}{2}\right) \right).$$

Since $U_D \in SU(2)$, $|z| = 1$. The relative phase change induced by this holonomy is

$$\phi = \arg(z/z^*) \in (-\pi, \pi]. \tag{3.2}$$

That the range of ϕ is always $(-\pi, \pi]$ is not necessarily obvious. To motivate our assertion we sketch a proof. We have that (writing $z/z^* =: w$) in general $\arg(w) = \text{atan2}(\text{Im}(w), \text{Re}(w))$. atan2 is either $\pm\pi/2$ or a function of $\text{Im}(w)/\,\text{Re}(w)$ that maps $\mathbb{R}$ to $(-\pi, \pi]$. For $\varphi \in [0, 2\pi)$ $\text{Im}(w)/\,\text{Re}(w)$ diverges with the left and right limits being either $\pm\infty$ (this can be seen by plotting the function for different values of m). Notwithstanding the diverging points, the rest of $\text{Im}(w)/\,\text{Re}(w)$ is continuous. Because the positive and negative divergent points alternate the range of the argument is $(-\pi, \pi]$.

3.3. Rotation gates

The gate specified by (3.1) is also the rotation gate in the z direction. A relative phase change of ϕ is the same as a rotation of our state by $-\phi$ (up to a global phase, which is irrelevant). We can also interpret the gate as a passive rotation (a rotation of our measurement basis) by ϕ, instead of an active rotation of our state. This makes intuitive sense because when we project into a different subspace we are effectively rotating our basis. Therefore, (3.1) is a mapping that tells us how a rotation of a subspace in which we project a state relates to a rotation of the state itself.

At first, finding rotation gates in the x and y directions seems complicated. However, we can simply convert our rotation operator along the z direction to two new rotation operators along the other axes by changing our basis. Recall that a matrix can be represented in other basis through (where P is the basis transformation matrix) $A' = PAP^{-1}$. So, we have $\mathcal{D}_x(\phi) = \mathcal{D}_y(\pi/2)\mathcal{D}_z(\phi)\mathcal{D}_y(\pi/2)^{-1}$ and $\mathcal{D}_y(\phi) = \mathcal{D}_x(3\pi/2)\mathcal{D}_z(\phi)\mathcal{D}_x(3\pi/2)^{-1}$. This gives for the rotation gates

$$U_{D,x} = \frac{1}{\sqrt{\cos^{2+4m}\left(\frac{\varphi}{2}\right) + \sin^{2+4m}\left(\frac{\varphi}{2}\right)}} \begin{pmatrix} \text{Re}(z) & i\,\text{Im}(z) \\ i\,\text{Im}(z) & \text{Re}(z) \end{pmatrix},$$

$$U_{D,y} = \frac{1}{\sqrt{\cos^{2+4m}\left(\frac{\varphi}{2}\right) + \sin^{2+4m}\left(\frac{\varphi}{2}\right)}} \begin{pmatrix} \text{Re}(z) & -\text{Im}(z) \\ \text{Im}(z) & \text{Re}(z) \end{pmatrix}.$$

These matrices are equivalent to the following list of angles by which we rotate our subspaces. They are:

$$U_{D,x} = \mathcal{D}_x(\phi) : (0,0) \to \left(\frac{\pi}{2}, \pi\right) \to \left(\varphi, \frac{\pi}{2}\right) \to (0,0),$$

$$U_{D,y} = \mathcal{D}_y(\phi) : (0,0) \to \left(\varphi, \begin{matrix} 0 \text{ if } m \text{ is even} \\ \pi \text{ if } m \text{ is odd} \end{matrix}\right) \to \left(\frac{\pi}{2}, \frac{\pi}{2}\right) \to (0,0),$$

$$U_{D,z} = \mathcal{D}_z(\phi) : (0,0) \to \left(\frac{\pi}{2}, \pi\right) \to \left(\frac{\pi}{2}, \varphi\right) \to (0,0),$$

where φ can be found by solving (3.2).

3.4. CNOT gate

To achieve a universal set of quantum gates we need to construct the CNOT gate. In principle we could extend the scheme for single-qubit gates directly, by defining frames as $|J, M\rangle$ (with J the total angular momentum and M the total-angular-momentum projection quantum number),

$$\left\{e^{-i\theta J_y}e^{-i\phi J_z}\,|J,\pm J\rangle\,, e^{-i\theta J_y}e^{-i\phi J_z}\,|J,0\rangle\,, e^{-i\theta J_y}e^{-i\phi J_z}\,|0,0\rangle\right\}.$$

We then pick either the control or target qubit to have half-odd integer spin and the remaining qubit to have integer spin (so the total spin is half-odd integer and the overlap matrix admits a unique polar decomposition) and once again try to find the appropriate measurement sequence. We call this an 'active' CNOT gate.

Experimentally, it is easier to implement a 'passive' CNOT gate, where we embed our single-qubit gate into a larger system. We use a similar scheme as [16]. Suppose our states have an extra degree of freedom, other than angular momentum, labeled by ℓ. This degree of freedom will act as our control qubit. We can prepare a beam of particles of the form $a\,|j,\ell\rangle + b\,|j,\ell'\rangle + c\,|-j,\ell\rangle + d\,|-j,\ell'\rangle$, with $|a|^2 + |b|^2 + |c|^2 + |d|^2 = 1$. As illustrated in figure 3.1, we send this particle beam through a filtration device (akin to a polarizing beam splitter). Let $|0\rangle$ and $|1\rangle$ represent the interferometer arms. The state after the filtration device will be

$$|\Psi_k\rangle = (a\,|j,\ell\rangle + c\,|-j,\ell\rangle) \otimes |0\rangle + (b\,|j,\ell'\rangle + c\,|-j,\ell'\rangle) \otimes |1\rangle\,.$$

In the 0 arm we expose the beam to a single-qubit X gate (where we make the sequence of measurements), while in the 1 arm we do nothing. We then recombine the beams. The output will be of the form $a\,|-j,\ell\rangle + b\,|j,\ell'\rangle + c\,|j,\ell\rangle + d\,|-j,\ell'\rangle$. We see that this setup corresponds to the action of a CNOT gate.

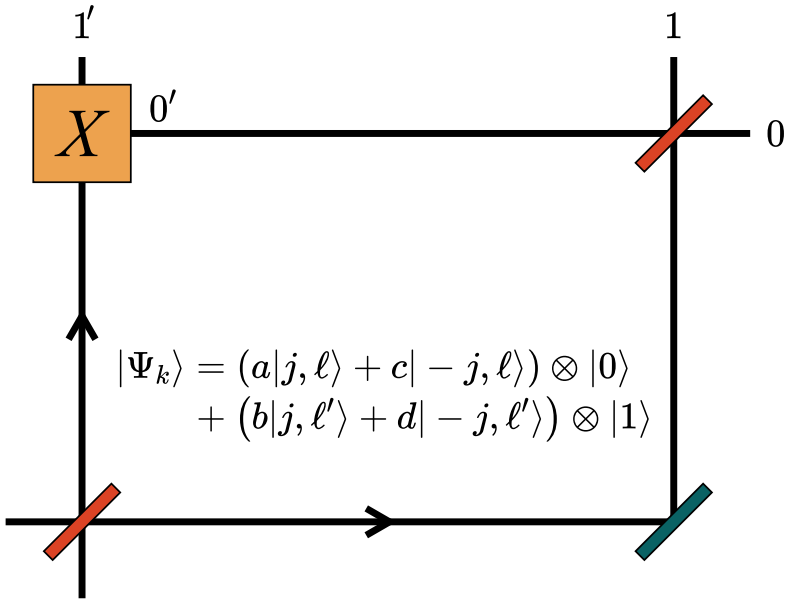

Figure 3.1: A passive CNOT gate, following a similar scheme as [16]. A filtration device splits the input state. In the 0 arm we implement a single-qubit X gate while in the 1 arm we do nothing. The states are then recombined.

3.5. Toffoli gate

Instead of single-qubit gates and the CNOT gate, we can also achieve universality by only using the Toffoli gate [7]. The Toffoli gate acts on three qubits at once. We will show that our scheme unfortunately does

not generalize (at least not naively) to a three-qubit system. Suppose we have three angular momentum coherent states, which we denote with $|j, j', j''\rangle$. We can span the three qubit system with the following set of frames:

$$\left\{e^{-i\theta J_y}e^{-i\phi J_z}\left|j,j,j\right\rangle, e^{-i\theta J_y}e^{-i\phi J_z}\left|j,j,-j\right\rangle, e^{-i\theta J_y}e^{-i\phi J_z}\left|j,-j,j\right\rangle, e^{-i\theta J_y}e^{-i\phi J_z}\left|j,-j,-j\right\rangle,\right.$$
$$\left. e^{-i\theta J_y}e^{-i\phi J_z}\left|-j,j,j\right\rangle, e^{-i\theta J_y}e^{-i\phi J_z}\left|-j,j,-j\right\rangle, e^{-i\theta J_y}e^{-i\phi J_z}\left|-j,-j,j\right\rangle, e^{-i\theta J_y}e^{-i\phi J_z}\left|-j,-j,-j\right\rangle\right\}.$$

In this basis, the Toffoli gate takes one of three forms depending on which two qubits are the control qubits. If a generic state is $|j, j', j''\rangle$, then we have for j and j'; j' and j''; and j and j'' as control qubits, respectively,

$$\begin{pmatrix}1&0&0&0&0&0&0&0\\0&1&0&0&0&0&0&0\\0&0&1&0&0&0&0&0\\0&0&0&1&0&0&0&0\\0&0&0&0&1&0&0&0\\0&0&0&0&0&1&0&0\\0&0&0&0&0&0&0&1\\0&0&0&0&0&0&1&0\end{pmatrix}, \quad \begin{pmatrix}1&0&0&0&0&0&0&0\\0&1&0&0&0&0&0&0\\0&0&1&0&0&0&0&0\\0&0&0&0&0&0&0&1\\0&0&0&0&1&0&0&0\\0&0&0&0&0&1&0&0\\0&0&0&0&0&0&1&0\\0&0&0&1&0&0&0&0\end{pmatrix}, \quad \begin{pmatrix}1&0&0&0&0&0&0&0\\0&1&0&0&0&0&0&0\\0&0&1&0&0&0&0&0\\0&0&0&1&0&0&0&0\\0&0&0&0&1&0&0&0\\0&0&0&0&0&0&0&1\\0&0&0&0&0&0&1&0\\0&0&0&0&0&1&0&0\end{pmatrix}.$$

Just like the single-qubit system we can measure $\left(\vec{n}\cdot\vec{J}\right)^2$ to project into frames spanned by

$$\begin{aligned}
e^{-i\theta J_y}e^{-i\phi J_z}\left|3j,3j\right\rangle &= e^{-i\theta J_y}e^{-i\phi J_z}\left|j,j,j\right\rangle,\\
e^{-i\theta J_y}e^{-i\phi J_z}\left|3j,j\right\rangle &= \frac{e^{-i\theta J_y}e^{-i\phi J_z}}{\sqrt{3}}(\left|j,j,-j\right\rangle+\left|j,-j,j\right\rangle+\left|-j,j,j\right\rangle),\\
e^{-i\theta J_y}e^{-i\phi J_z}\left|3j,-j\right\rangle &= \frac{e^{-i\theta J_y}e^{-i\phi J_z}}{\sqrt{3}}(\left|j,-j,-j\right\rangle+\left|-j,j,-j\right\rangle+\left|-j,-j,j\right\rangle),\\
e^{-i\theta J_y}e^{-i\phi J_z}\left|3j,-3j\right\rangle &= e^{-i\theta J_y}e^{-i\phi J_z}\left|-j,-j,-j\right\rangle,\\
e^{-i\theta J_y}e^{-i\phi J_z}\left|j,j\right\rangle_A &= \frac{e^{-i\theta J_y}e^{-i\phi J_z}}{\sqrt{3}}\left(\sqrt{2}\left|j,j,-j\right\rangle-\frac{1}{\sqrt{2}}\left|j,-j,j\right\rangle-\frac{1}{\sqrt{2}}\left|-j,j,j\right\rangle\right),\\
e^{-i\theta J_y}e^{-i\phi J_z}\left|j,-j\right\rangle_A &= \frac{e^{-i\theta J_y}e^{-i\phi J_z}}{\sqrt{3}}\left(-\sqrt{2}\left|-j,-j,j\right\rangle+\frac{1}{\sqrt{2}}\left|j,-j,-j\right\rangle+\frac{1}{\sqrt{2}}\left|-j,j,-j\right\rangle\right),\\
e^{-i\theta J_y}e^{-i\phi J_z}\left|j,j\right\rangle_B &= \frac{e^{-i\theta J_y}e^{-i\phi J_z}}{\sqrt{2}}(\left|j,-j,j\right\rangle-\left|-j,j,j\right\rangle),\\
e^{-i\theta J_y}e^{-i\phi J_z}\left|j,-j\right\rangle_B &= \frac{e^{-i\theta J_y}e^{-i\phi J_z}}{\sqrt{2}}(\left|j,-j,-j\right\rangle-\left|-j,j,-j\right\rangle).
\end{aligned}$$

Note that this makes clear that the three-qubit space is a direct sum of three subspaces. The basis transformation matrix from the $|j, j', j''\rangle$ basis to the $|J, J'\rangle$ basis is given by

$$S=\begin{pmatrix}1&0&0&0&0&0&0&0\\0&\frac{1}{\sqrt{3}}&0&0&\sqrt{\frac{2}{3}}&0&0&0\\0&\frac{1}{\sqrt{3}}&0&0&-\frac{1}{\sqrt{6}}&0&\frac{1}{\sqrt{2}}&0\\0&0&\frac{1}{\sqrt{3}}&0&0&\frac{1}{\sqrt{6}}&0&\frac{1}{\sqrt{2}}\\0&\frac{1}{\sqrt{3}}&0&0&-\frac{1}{\sqrt{6}}&0&-\frac{1}{\sqrt{2}}&0\\0&0&\frac{1}{\sqrt{3}}&0&0&\frac{1}{\sqrt{6}}&0&-\frac{1}{\sqrt{2}}\\0&0&\frac{1}{\sqrt{3}}&0&0&-\sqrt{\frac{2}{3}}&0&0\\0&0&0&1&0&0&0&0\end{pmatrix}.$$

Operators transform as (new) $= S^\dagger$(old)S. So, in the $|J, J'\rangle$ basis the Toffoli gates are given by

$$\begin{pmatrix} 1 & 0 & 0 & 0 & 0 & 0 & 0 & 0 \\ 0 & 1 & 0 & 0 & 0 & 0 & 0 & 0 \\ 0 & 0 & \frac{2}{3} & \frac{1}{\sqrt{3}} & 0 & \frac{\sqrt{2}}{3} & 0 & 0 \\ 0 & 0 & \frac{1}{\sqrt{3}} & 0 & 0 & -\sqrt{\frac{2}{3}} & 0 & 0 \\ 0 & 0 & 0 & 0 & 1 & 0 & 0 & 0 \\ 0 & 0 & \frac{\sqrt{2}}{3} & -\sqrt{\frac{2}{3}} & 0 & \frac{1}{3} & 0 & 0 \\ 0 & 0 & 0 & 0 & 0 & 0 & 1 & 0 \\ 0 & 0 & 0 & 0 & 0 & 0 & 0 & 1 \end{pmatrix}, \quad \begin{pmatrix} 1 & 0 & 0 & 0 & 0 & 0 & 0 & 0 \\ 0 & 1 & 0 & 0 & 0 & 0 & 0 & 0 \\ 0 & 0 & \frac{2}{3} & \frac{1}{\sqrt{3}} & 0 & \frac{1}{3\sqrt{2}} - \frac{\sqrt{2}}{3} & 0 & -\frac{1}{\sqrt{6}} \\ 0 & 0 & \frac{1}{\sqrt{3}} & 0 & 0 & \frac{1}{\sqrt{6}} & 0 & \frac{1}{\sqrt{2}} \\ 0 & 0 & 0 & 0 & 1 & 0 & 0 & 0 \\ 0 & 0 & \frac{1}{3\sqrt{2}} - \frac{\sqrt{2}}{3} & \frac{1}{\sqrt{6}} & 0 & \frac{5}{6} & 0 & -\frac{1}{2\sqrt{3}} \\ 0 & 0 & 0 & 0 & 0 & 0 & 1 & 0 \\ 0 & 0 & -\frac{1}{\sqrt{6}} & \frac{1}{\sqrt{2}} & 0 & -\frac{1}{2\sqrt{3}} & 0 & \frac{1}{2} \end{pmatrix},$$

$$\begin{pmatrix} 1 & 0 & 0 & 0 & 0 & 0 & 0 & 0 \\ 0 & 1 & 0 & 0 & 0 & 0 & 0 & 0 \\ 0 & 0 & \frac{2}{3} & \frac{1}{\sqrt{3}} & 0 & \frac{1}{3\sqrt{2}} - \frac{\sqrt{2}}{3} & 0 & \frac{1}{\sqrt{6}} \\ 0 & 0 & \frac{1}{\sqrt{3}} & 0 & 0 & \frac{1}{\sqrt{6}} & 0 & -\frac{1}{\sqrt{2}} \\ 0 & 0 & 0 & 0 & 1 & 0 & 0 & 0 \\ 0 & 0 & \frac{1}{3\sqrt{2}} - \frac{\sqrt{2}}{3} & \frac{1}{\sqrt{6}} & 0 & \frac{5}{6} & 0 & \frac{1}{2\sqrt{3}} \\ 0 & 0 & 0 & 0 & 0 & 0 & 1 & 0 \\ 0 & 0 & \frac{1}{\sqrt{6}} & -\frac{1}{\sqrt{2}} & 0 & \frac{1}{2\sqrt{3}} & 0 & \frac{1}{2} \end{pmatrix}.$$

From section 2.3 we know that any gate will be the product of the overlap matrices. Since our three-qubit system decomposes into three independent vector spaces, the overlap matrices will be block diagonal,

$$(\mathcal{F}_a|\mathcal{F}_b) = \begin{pmatrix} F_1 & 0 & 0 \\ 0 & F_2 & 0 \\ 0 & 0 & F_2 \end{pmatrix},$$

with F_1 the 4×4 overlap matrix for the vector space corresponding to a total angular momentum of $3j$, and F_2 the 2×2 overlap matrix for the vector space corresponding to a total angular momentum of j. All three of the Toffoli gates in the $|J, J'\rangle$ basis require mixing of the three vector spaces. This cannot be realized with products of overlap matrices. Hence, we cannot produce the Toffoli gate.

Although these bases do not allow for the Toffoli gate, there may exist other bases (coupled to observables) that do. What these bases are, and even whether they exist is still an open question.

3.6. Universal quantum computation for j = 3/2

It is instructive to work out the discrete set of gates needed for universal quantum computation in the case of $j = 3/2$. The process for working out higher-j gate is identical. Our goal is to construct the H, S, T, and Pauli gates. For that, we need ϕ, and to calculate ϕ we first need $U_{D,z}$. Plugging in $m = 1$ into (3.1) gives us

$$U_{D,z}^{(j=3/2)} = \frac{1}{\sqrt{10 + 6\cos(2\varphi)}} \begin{pmatrix} 1 + 3e^{-2i\varphi} & 0 \\ 0 & 1 + 3e^{2i\varphi} \end{pmatrix}.$$

Therefore,

$$\phi = \arg\left(\frac{1 + 3e^{-2i\varphi}}{1 + 3e^{2i\varphi}}\right). \tag{3.3}$$

A plot of (3.3) is shown in figure 3.2. Note that ϕ is multivalued. However, in the end, each intersection point yields the same holonomy. We should clarify that by same we mean up to a global phase; for the rest of this section if a gate is equal, equality up to a global phase is meant. Of course, a global phase is not measurable and does not have any effect on the quantum system.

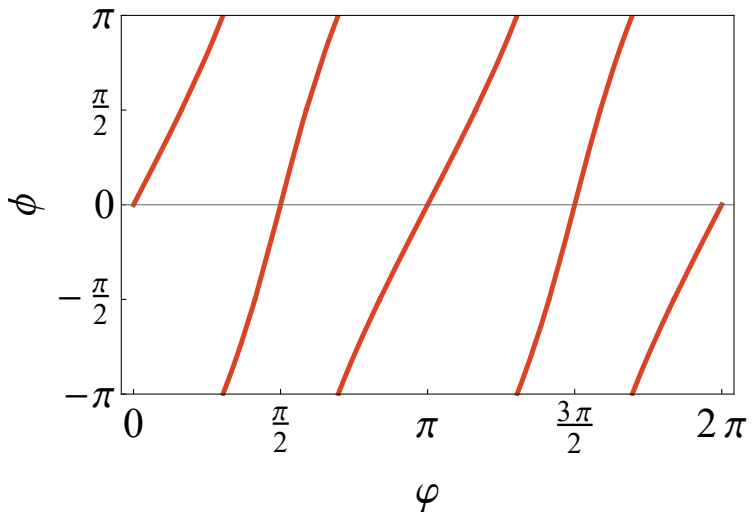

Figure 3.2: The relative phase ϕ as a function of the rotation of the subspace rotation φ for $j = 3/2$.

For the T, S and Pauli gates we want to find the intersection point where ϕ is $\pi/4$, $\pi/2$ and π, respectively. We find the gates can be made using the following sequence of measurements:

$$T : (0,0) \to \left(\frac{\pi}{2}, \pi\right) \to \left(\frac{\pi}{2}, 2\,\text{arcsec}\left(2\sqrt{\frac{6}{\sqrt{6\left(\sqrt{2}-\sqrt{36\sqrt{2}+70}+10\right)}+12}}\right) \approx 1.44\right) \to (0,0),$$

$$S : (0,0) \to \left(\frac{\pi}{2}, \pi\right) \to \left(\frac{\pi}{2}, \arctan\left(\frac{3+\sqrt{17}}{2}\right) \approx 1.30\right) \to (0,0),$$

$$X : (0,0) \to \left(\frac{\pi}{2}, \pi\right) \to \left(\arctan\left(\sqrt{2}\right) \approx 0.955, \frac{\pi}{2}\right) \to (0,0),$$

$$Y : (0,0) \to \left(\arctan\left(\sqrt{2}\right), \pi\right) \to \left(\frac{\pi}{2}, \frac{\pi}{2}\right) \to (0,0),$$

$$Z : (0,0) \to \left(\frac{\pi}{2}, \pi\right) \to \left(\frac{\pi}{2}, \arctan\left(\sqrt{2}\right)\right) \to (0,0).$$

Note that these sequences are not unique. For example, the Z gate is also given by a measurement sequence where the second pair of angles is replaced by $(\pi/2, 0)$. Next is the Hadamard gate. H can be decomposed into two rotations, a π rotation around the z axis and a $\pi/2$ rotation around the y axis. We can use the values we found above to construct the following sequence,

$$H : (0,0) \to \left(\arctan\left(\frac{3+\sqrt{17}}{2}\right), \pi\right) \to \left(\frac{\pi}{2}, \frac{\pi}{2}\right) \to (0,0) \to \left(\frac{\pi}{2}, \pi\right) \to \left(\frac{\pi}{2}, \arctan\left(\sqrt{2}\right)\right) \to (0,0).$$

With the above gates we can achieve universal single-qubit computation. If we embed the X gate into the setup described in section 3.4 we can achieve universal quantum computation.

3.7. Gate efficacy

Having constructed the formalism to describe holonomic quantum gates, we now turn to their performance. There are two main mechanisms that give rise to faults in the gates' performance. The first is that with each projection into a subspace p, there is a chance our state will collapse into the orthogonal subspace

$p^{\perp}$ instead. The second is purely experimental: in practice it is difficult to project perfectly into a given subspace. We will have some small error $\delta\theta$ and $\delta\phi$ in our angles.

Let us start with the probability amplitudes. In this case the gate itself works perfectly, but we have to take into account post-selection of the states. Recall from section 2.1 that the transition probability for a series of projections $\Gamma_{\mathcal{C}} = P_m \dots P_1$ is given by $\langle\psi|P_1 \dots P_{m-1} P_m P_{m-1} \dots P_1|\psi\rangle$. Because our initial and final frame is the same, it is convenient to look at the matrix representation of $\Gamma_{\mathcal{C}}$ in the $\{|\pm j\rangle\}$ basis. Then, all computations reduce to linear algebra. The representation is given by

$$\Gamma_{\mathcal{C}} \xrightarrow{\text{represented by}} (\mathcal{F}_0|\mathcal{F}_m)(\mathcal{F}_m|\mathcal{F}_{m-1}) \dots (\mathcal{F}_1|\mathcal{F}_0).$$

We can write an arbitrary state this basis as $|\psi\rangle = \cos\left(\frac{a}{2}\right)|j\rangle + e^{ib}\sin\left(\frac{a}{2}\right)|-j\rangle$, with $a \in [0, \pi]$ and $b \in [0, 2\pi)$.

We will focus on the rotation gates since they form the basis for all single-qubit gates. Furthermore, due to symmetry, we only need to look at rotations around the z axis. It turns out that the transition amplitude $T_{\mathcal{C}}$ is independent of the input state and is given by

$$T_{\mathcal{C}} = 4^{-2m}\left(\cos^{2+4m}\left(\frac{\varphi}{2}\right) + \sin^{2+4m}\left(\frac{\varphi}{2}\right)\right).$$

A plot is shown in figure 3.3. We can see that as we increase j, the transition amplitude decreases exponentially. The maxima of the transition amplitude occur at integer multiples of π, while the minima occur at half-integer multiples of π. If we compare this to figure 3.2, we see that for both cases the extrema correspond to no relative phase change at all. However, at half-integer multiples of π the state acquires a global phase of -1, while for integer multiples of π the global phase remains zero. For $j = 3/2$ the maximum value of the transition amplitude is $1/16 \approx 0.063$, while the minimum value is $1/64 \approx 0.016$. All in all this plot tells us that we should pick j to be as low as possible to have a feasible gate.

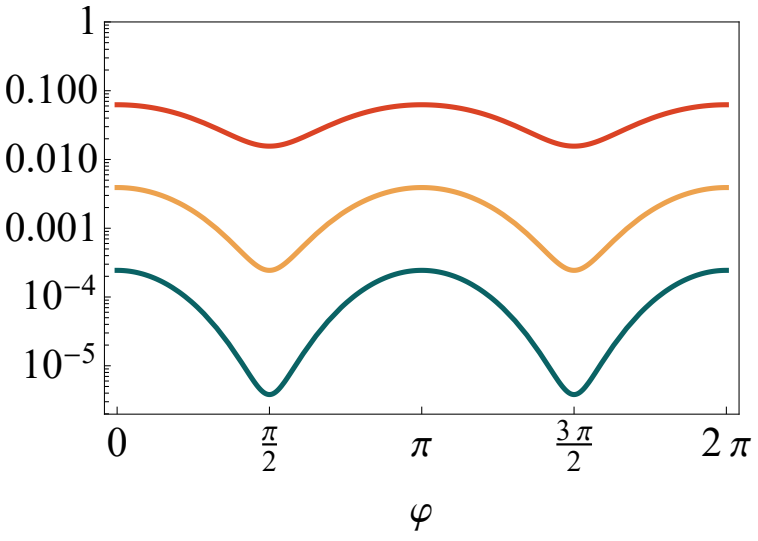

Figure 3.3: A logarithmic plot of the transition amplitude for rotations along the z axis as a function of the subspace rotation φ. Red is $j = 3/2$, yellow is $j = 5/2$, and blue is $j = 7/2$.

Next, we would like to know what happens when we perturb our subspace angles. Our perturbed state will acquire a slightly different holonomy (U'_D) than the unperturbed state (U_D). We will quantify the difference in holonomy by calculation the minimum fidelity over all possible input states $|\psi\rangle$,

$$F(\psi', \psi) = \min_{|\psi\rangle \in \mathcal{F}_1} \left|\langle\psi|U_D'^{\dagger} U_D|\psi\rangle\right|^2.$$

We assume $\varphi = \arctan\sqrt{2} \approx 0.955$, the angle for a Z gate. Small perturbations will be in the order of 10^{-2}. In figure 3.4a and 3.4b we show surfaces of minimum fidelity corresponding to perturbations of the form $(\theta_2, \phi_2) \to (\theta_2 + \delta\theta, \phi_2 + \delta\phi)$ and $(\theta_3, \varphi) \to (\theta_3 + \delta\theta, \varphi + \delta\phi)$, respectively.

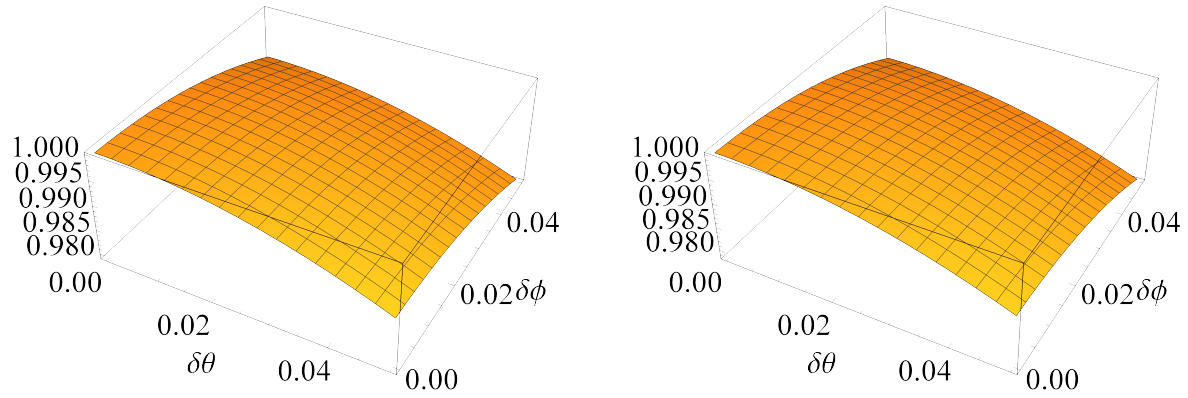

(a) Perturbations of the form $(\theta_2 + \delta\theta, \phi_2 + \delta\phi)$.

(b) Perturbations of the form $(\theta_3 + \delta\theta, \varphi + \delta\phi)$.

Figure 3.4: Surface of minimum fidelity for small perturbations away from the Z gate.

We can see that the gates are robust, that is, they are fairly insensitive towards noise. There is effectively no difference whether we consider perturbations of the second measurement or of the third measurement. We could have expected this, by symmetry of our measurement path. We would also like to see if this robustness changes when we change j. To that end, we only perturb φ. This is shown in figure 3.5.

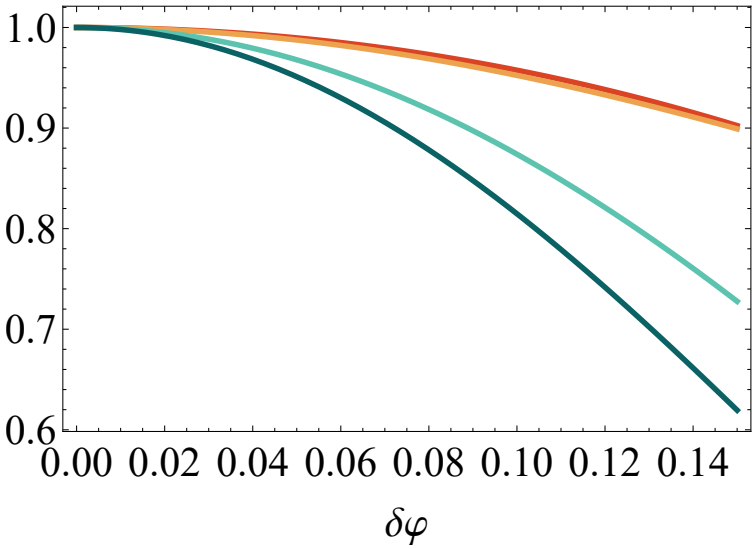

Figure 3.5: The minimum fidelity for perturbations of the form $(\varphi + \delta\varphi)$ of the Z gate. Red is $j = 3/2$, yellow is $j = 5/2$, cyan is $j = 7/2$ and blue is $j = 9/2$.

We can see that for small perturbations the value of j is irrelevant. However, for larger perturbations the lower j-gates have higher fidelity. Interestingly, the difference between $j = 3/2$ and $j = 5/2$ is very small, especially compared to $j = 7/2$ and higher. We do not know of a good explanation for this.

The general shape and trend of the curves are not changed by much if we perturb the first measurement and then plot the effect of a perturbation of the second measurement. The main features discussed above remain essentially the same, except that the fidelity is slightly lower.

From the above analyses we conclude that the best gates are for low values of j. Although a $j = 5/2$ gate will have a similar resilience to errors as a $j = 3/2$ gate, the difference in transition amplitude decreases exponentially, making the latter a more attractive option.

3.8. The Zeno limit

We conclude our discussion on discrete holonomic gates by verifying the Zeno limit. We will take the Zeno limit for the $\mathcal{D}_z(\phi)$ gate. As there is some freedom in what measurement sequence to take, we pick $(0,0) \to \left(\frac{\pi}{2}, 0\right) \to \left(\frac{\pi}{2}, \varphi\right) \to (0,0)$ for simplicity. The continuous-path holonomy for a curve parametrized by $s \in [0,1]$ is given by [17]

$$U_D = U_{0,1} \mathrm{P} e^{\int_0^1 \mathrm{d}s A(s)},$$

where P denotes path ordering and $[A(s)]_{k,l} := \langle \dot{a}_k(s) | a_l(s) \rangle$, with $\{a_k(s)\}_{k=1}^2$ a smooth set of frames. $U_{0,1}$ is the overlap matrix of the first and final frame [10]. Because we have a closed path $U_{0,1} = I$. Furthermore,

$$\begin{aligned}
|a_0(s)\rangle &= e^{-i\phi(s)J_z} e^{-i\theta(s)J_y} |j\rangle, \\
|\dot{a}_0(s)\rangle &= -i\Big(\dot{\phi}(s) e^{-i\phi(s)J_z} J_z e^{-i\theta(s)J_y} + \dot{\theta}(s) e^{-i\phi(s)J_z} J_y e^{-i\theta(s)J_y}\Big) |j\rangle, \\
|a_1(s)\rangle &= e^{-i\phi(s)J_z} e^{-i\theta(s)J_y} |-j\rangle, \\
|\dot{a}_1(s)\rangle &= -i\Big(\dot{\phi}(s) e^{-i\phi(s)J_z} J_z e^{-i\theta(s)J_y} + \dot{\theta}(s) e^{-i\phi(s)J_z} J_y e^{-i\theta(s)J_y}\Big) |-j\rangle,
\end{aligned}$$

where dots denote derivatives with respect to s. We then find that $A(s) = i\dot{\phi} j \sigma_z$. So, the continuous holonomy is

$$U_D = \exp\left(ij\sigma_z \int_0^{\varphi} \mathrm{d}\phi\right) = \begin{pmatrix} e^{i\varphi j} & 0 \\ 0 & e^{-i\varphi j} \end{pmatrix} \sim \begin{pmatrix} 1 & 0 \\ 0 & e^{-2i\varphi j} \end{pmatrix},$$

where the final identification holds because a global phase is not measurable.

Suppose we have $j = 3/2$ and rotate our subspace by $\varphi = \pi/4$. In the Zeno limit our holonomy should be a phase shift with argument $-2 \times 3\pi/(2 \times 4) = -3\pi/4 \approx -2.35$. How do we take the appropriate limit in the discrete case? It turns out we have to increase the number of measurements like shown in figure 3.6.

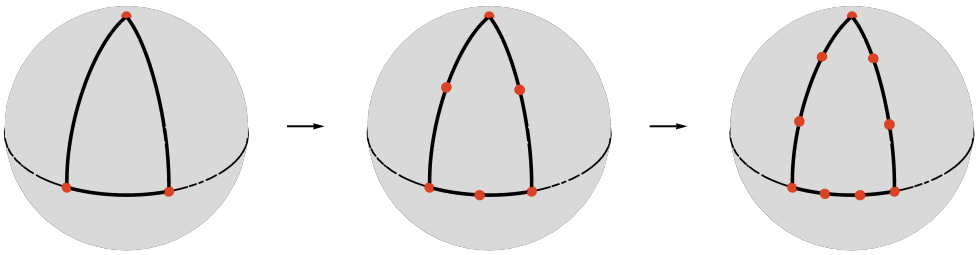

Figure 3.6: We approach the Zeno limit by making more measurements along the path.

To see this, note that we want to make the measurement sequence $(0,0) \to \left(\frac{\pi}{2}, 0\right) \to \left(\frac{\pi}{2}, \varphi\right) \to (0,0)$ more and more dense. This sequence is composed out of three legs: one leg down, one leg along the equator, and

one leg back up again. A first guess would be to add measurements points by first dividing each leg into two, then adding a point half way. Next, divide the leg into three and add two points. We keep dividing more and more finely until we effectively have a smooth path. This works well for the first two legs, but for the last leg there is an ambiguity. Intuitively, we want to stay on the geodesic when dividing the path. Otherwise, we would twist around the sphere when going back up to the pole. This would change the character of the holonomy. So, when we go from $\left(\frac{\pi}{2}, \varphi\right) \to (0,0)$ we keep our ϕ coordinate fixed to φ. Only in the last measurement we 'jump' from φ to zero. Does this jump matter?

The answer is no. The easiest way to see this is to look at the matrices that make up the holonomy U_D. If we do not include the jump we will have a matrix of the form

$$U_D \propto ((0,0)|(\theta_m,\varphi)) \times ((\theta_m,\varphi)|(\theta_{m-1},\varphi)) \times \cdots \times ((\theta_2,0)|(0,0)). \tag{3.4}$$

If we include the jump our matrix will look like

$$U_D \propto ((0,0)|(0,\varphi)) \times ((0,\varphi)|(\theta_m,\varphi)) \times ((\theta_m,\varphi)|(\theta_{m-1},\varphi)) \times \cdots \times ((\theta_2,0)|(0,0)). \tag{3.5}$$

However,

$$\begin{aligned}((0,0)|(0,\varphi)) \times ((0,\varphi)|(\theta_m,\varphi)) &= \begin{pmatrix} e^{-\frac{i}{2}(2m+1)\varphi} & 0 \\ 0 & e^{\frac{i}{2}(2m+1)\varphi} \end{pmatrix} \times \begin{pmatrix} \cos^{2m+1}\left(\frac{\theta_m}{2}\right) & -\sin^{2m+1}\left(\frac{\theta_m}{2}\right) \\ \sin^{2m+1}\left(\frac{\theta_m}{2}\right) & \cos^{2m+1}\left(\frac{\theta_m}{2}\right) \end{pmatrix} \\ &= ((0,0)|(\theta_m,\varphi)).\end{aligned}$$

So, there is no difference between (3.4) and (3.5). Another way of viewing this is by nothing that projectors are gauge-invariant, and that all subspace at the north pole are connected by a $U(1)$ gauge transformation. So, the sequence of projection into different subspace of the north pole should not matter. The appropriate way to take the Zeno limit, then, is to increasingly make the measurement sequence more dense along the geodesic connecting the initial four measurement points.

If we choose the initial state, say $|\psi\rangle = \frac{1}{\sqrt{2}}(|j\rangle + |-j\rangle)$, we can also calculate the transition probability. This probability should go to one as the amount of measurements increases, because of the quantum Zeno effect. Furthermore, the off-diagonal elements of the holonomy U_D should go to zero and the argument of the relative phase shift of the diagonal elements should go to $-3\pi/4$. This is plotted in figure 3.7.

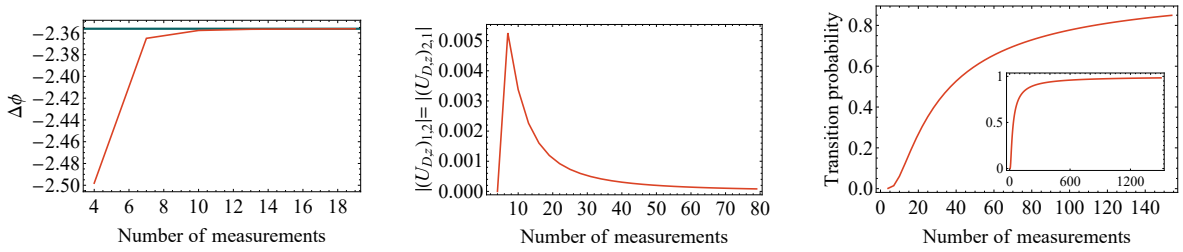

Figure 3.7: The behavior of the discrete holonomy U_D for a subspace rotation of $\varphi = \pi/4$ (using a Z-gate) when the amount of measurements is increased. (left) The argument of the relative phase of the diagonal elements of the holonomy. (center) The absolute value of the off-diagonal elements of the holonomy. (right) The transition probability for an initial state $\frac{1}{\sqrt{2}}(|j\rangle + |-j\rangle)$. The inset shows a zoomed-out version of the larger plot.

In figure 3.7 we can see that the diagonal elements quickly approach the limiting value. However, the off-diagonal elements take longer to go zero (the initial spike is because with only four measurements U_D is diagonal). Approaching a transition amplitude of one takes the longest of all (as can be seen from the inset, where the amount of measurements exceeds 1000). To sum up, when we increase the amount of measurements we reassuringly recover the expected continuous-path holonomy, which, unlike the discrete holonomy, is Abelian.

Chapter 4
Conclusion

We have demonstrated that interferometry-based discrete holonomic quantum computation can achieve universality. In particular, we have explicitly constructed quantum gates for the angular-momentum coherent states, whereby rotation gates were achieved using a sequence of four projective measurements. The procedure we have used to construct the quantum gates generalizes easily to different quantum states as well as multi-qubit systems. Like other holonomic quantum gates, our gates are resilient to errors. We also recover previously-found results for continuous-path holonomic quantum computation by taking the limit to infinitely many measurements.

Our work opens the way for experimental verification. It would be interesting to see how scalable our approach is. On more theoretical grounds it is worth investigating whether there exists states other than the angular-momentum coherent states that can be used in our experiment. And, if so, what performance difference those states would give. A worthwhile family of states to investigate are the subspaces spanned by the eigenkets of $J_{\vec{n}}$ where $m = \pm\frac{1}{2}$. In those cases the holonomy in the Zeno limit remains off-diagonal, and therefore retains its non-Abelian character. In what way the discrete case transitions to the continuous case is still an open question.

References

[1]M. V. Berry, "Quantal phase factors accompanying adiabatic changes", Proc. R. Soc. Lond. Ser. A **392**, 45–57 (1984).

[2]F. Wilczek and A. Zee, "Appearance of gauge structure in simple dynamical systems", Phys. Rev. Lett. **52**, 2111–2114 (1984).

[3]P. Zanardi and M. Rasetti, "Holonomic quantum computation", Phys. Lett. A **264**, 94–99 (1999).

[4]K. Nagata, K. Kuramitani, Y. Sekiguchi, and H. Kosaka, "Universal holonomic quantum gates over geometric spin qubits with polarised microwaves", Nature Comm. **9**, 3227 (2018).

[5]C. Zu, W. B. Wang, L. He, W. G. Zhang, C. Y. Dai, F. Wang, and L. M. Duan, "Experimental realization of universal geometric quantum gates with solid-state spins", Nature **514**, 72–75 (2014).

[6]D. K. L. Oi, "Unitary holonomies by direct degenerate projections", Phys. Rev. A **89**, 050102 (2014).

[7]M. A. Nielsen and I. L. Chuang, *Quantum computation and quantum information: 10th anniversary edition* (Cambridge University Press, 2016).

[8]J. Anandan and A. Pines, "Non-Abelian geometric phase from incomplete quantum measurements", Phys. Lett. A **141**, 335–339 (1989).

[9]C. A. Mead, "'"Block diagonalization" as generalization of Pancharatnam-Berry phase relation for multidimensional spaces", Phys. Rev. A **44**, 1473–1476 (1991).

[10]E. Sjöqvist, D. Kult, and J. Åberg, "Manifestations of quantum holonomy in interferometry", Phys. Rev. A **74**, 062101 (2006).

[11]D. Bhaumik, T. Nag, and B. Dutta-Roy, "Coherent states for angular momentum", J. Phys. A: Math. Gen. **8**, 1868–1874 (1975).

[12]J. J. Sakurai and J. Napolitano, *Modern quantum mechanics*, 2nd ed. (Cambridge University Press, 2017), pp. 168–172.

[13]Y. Aharonov and M. Vardi, "Meaning of an individual "Feynman path"", Phys. Rev. D **21**, 2235–2240 (1980).

[14]E. Sjöqvist, X. X. Yi, and J. Åberg, "Adiabatic geometric phases in hydrogenlike atoms", Phys. Rev. A **72**, 054101 (2005).

[15]A. Zee, "Non-Abelian gauge structure in nuclear quadrupole resonance", Phys. Rev. A **38**, 1–6 (1988).

[16]J. H. Lopes, W. C. Soares, B. de Lima Bernardo, D. P. Caetano, and A. Canabarro, "Linear optical CNOT gate with orbital angular momentum and polarization", Quantum Inf. Process. **18**, 256 (2019).

[17]D. Kult, J. Åberg, and E. Sjöqvist, "Noncyclic geometric changes of quantum states", Phys. Rev. A **74**, 022106 (2006).